Development of On-Line Reactivity Meter for Nuclear Reactors

Saleem A. Ansari

Abstract—**An on-line reactivity meter has been developed for continuous monitoring of reactivity in Pakistan Research Reactor-1 (PARR-1). The reactivity meter comprises two main parts. The first part is the hardware and software for on-line acquisition of neutron flux signals from plant instrumentation channels. The second part is high-level Fortran-77 real-time programming for the computation of reactivity by the solution of neutron kinetic equations. The PDP-11/23 plant computer is used for this purpose with time sharing of its regular data logging function. For PARR-2 reactor the reactivity meter is developed on an IBM PC/AT personal computer. The response of both reactivity meters is fast enough to monitor safety related reactivity and power excursions in the two reactors. The results of various reactivity measurements like reactivity coefficients, worth of control rods, and irradiation samples in PARR-1 using the reactivity meter are described. The proper choice and location of nuclear detectors and system calibration are also discussed.**

I. Introduction

THE advantages of using a reactivity meter in a reactor are manifold [1]. In the start-up and operation of nuclear reactors continuous reactivity surveillance is necessary to safely and efficiently reach the operating power level. At high power levels careful monitoring of reactivity is needed to determine the temperature, poison, and power coefficients of reactivity. The determination of the reactivity worth of the new fuel elements, reactor control systems, and the irradiated samples is also critical from reactor safety and control point of view.

There are two different techniques to measure the reactivity: dynamic and kinetic. In the dynamic technique the stable or asymptotic reactor period is measured and reactivity is determined from the in-hour equation. This technique works for positive periods only [2]. For the kinetic technique of measuring reactivity, reactivity changes may be made continuously and the reactivity at each instant determined by analyzing the time variation of the reactor power level using the point kinetics equations. The reactivity meter utilizes the kinetic method approach, which is described in the next section.

II. Theoretical Considerations

Point reactor kinetic equations give the time-dependent behavior of a reactor as [3], [4]

$$\frac{dP_{(t)}}{dt} = \frac{\beta}{l^*}\left[\frac{\rho_{(t)}}{\beta} - 1\right]P_{(t)} + \sum_{i=1}^{6}\lambda_i C_{i(t)} + S_{(t)} \quad (1)$$

Manuscript received October 19, 1990; revised February 1, 1991.

The author is with the Pakistan Institute of Nuclear Science and Technology, P.O. Nilore, Islamabad, Pakistan.

IEEE Log Number 9143437.

$$\frac{dC_i}{dt} = \frac{\beta_i}{l^*}P_{(t)} - \lambda_i C_i(t) \quad (2)$$

where

- $P_{(t)}$ reactor power at time t
- $\rho_{(t)}$ system reactivity
- $C_{i(t)}$ concentration of the delayed neutron precursors belonging to group i
- λ_i, β_i decay constant and fraction of delayed neutrons respectively for ith group
- l^* neutron mean lifetime in the reactor
- $S_{(t)}$ external neutron source.

The set of coupled differential equations can be reduced to a single integro-differential equation for $P_{(t)}$ which, in turn, can be rearranged as

$$\rho_{(t)} = \beta + \frac{1}{P_{(t)}}\frac{dP_{(t)}}{dt} - \frac{\beta}{P_{(t)}}\int_0^\infty D_{(u)}P_{(t-u)}\,du - \frac{l^*S_{(t)}}{\beta P_{(t)}} \quad (3)$$

where

$$D_{(u)} = \frac{1}{\beta}\sum_{i=1}^{6}\beta_i\lambda_i e^{-\lambda_i u}$$

is the delayed neutron kernel. $D(u)du$ is the probability that a delayed neutron will be emitted in du about u following a fission event at $u = 0$. Substituting the value of $D(u)$ in (3) and neglecting the source term one gets

$$\rho_{(t)} = \beta + \frac{l^*}{P_{(t)}}\frac{dP_{(t)}}{d_t} - \frac{l^*}{P_{(t)}}\sum_{i=1}^{6}\beta_i\lambda_i S_{i(t)} \quad (4)$$

where the term $S_{i(t)}$ describes the power history, i.e.,

$$S_{i(t)} = \int_0^\infty P_{(t-u)}e^{-\lambda_i u}\,du. \quad (5)$$

Putting $y = t - u$, $S_{i(t)}$ becomes

$$S_{i(t)} = e^{-\lambda_i t}\left[\int_{-\infty}^{0}P_{(y)}e^{\lambda_i y}\,dy + \int_0^t P_{(y)}e^{\lambda_i y}\,dy\right]. \quad (6)$$

Thus for small increments in time Δt,

$$S_{i(t1+\Delta t)} = e^{-\lambda_i \Delta t}\left[S_{i(t1)} + e^{-\lambda_i t1}\int_{t1}^{t_1+\Delta t}P_{(y)}e^{-\lambda_i y}\,dy\right]. \quad (7)$$

0018-9499/91/0800-0946$01.00

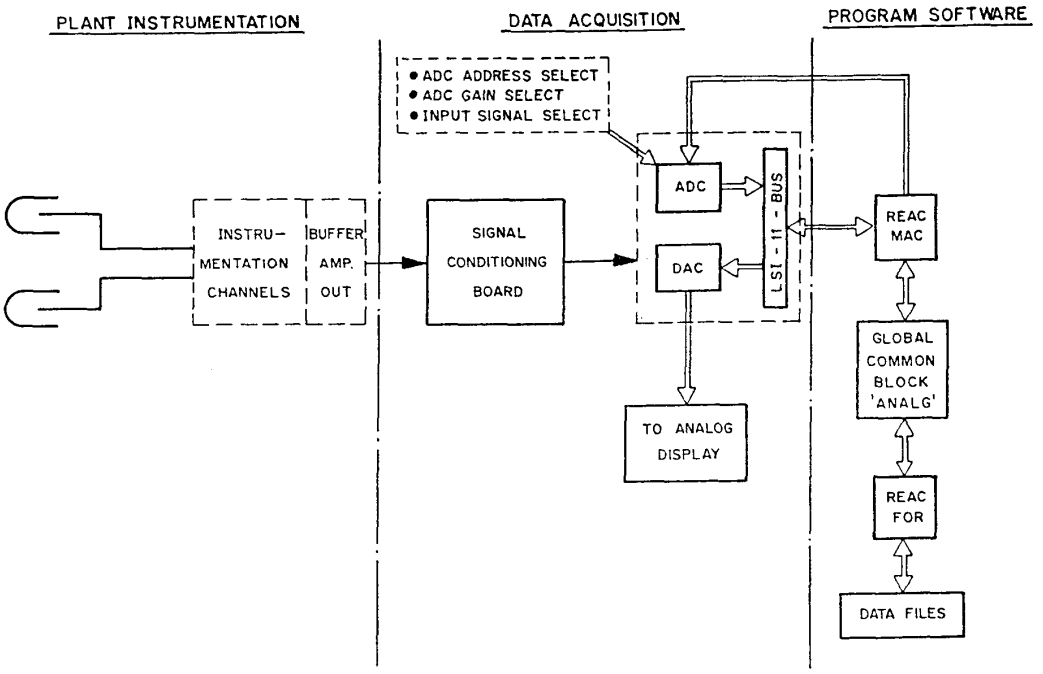

Fig. 1. Functional diagram of reactivity meter.

If we denote the power integral by R_i, i.e.,

$$R_i = \int_{t1}^{t1+\Delta t} P_{(y)} e^{\lambda_i y}\, dy, \tag{8}$$

we get

$$S_{i(t1+\Delta t)} = e^{-\lambda_i \Delta t}\left[S_{i(t1)} + R_i e^{-\lambda_i t1}\right]. \tag{9}$$

If the variation of $P_{(t)}$ is linear with time within a small interval of time Δt, it can be expressed by

$$P_{(y)} = P_{(y1)} + \frac{P_{(y1+\Delta t)} - P_{(y1)}}{\Delta t}\,(y - y1). \tag{10}$$

Substituting this value of $P_{(y)}$ in the integral R_i we get the source term as

$$S_{i(t1+\Delta t)} = S_{I(t1)} e^{-\lambda_i \Delta t} + \frac{1}{\lambda_i}\left(1 - e^{-\lambda_i \Delta t}\right) \cdot\left[P_{(t1)} - \frac{P_{(t1+\Delta t)} - P_{(t1)}}{\lambda_i \Delta t} + \frac{P_{(t1+\Delta t)} - P_{(t1)}}{\lambda_i}\right]. \tag{11}$$

Equation (11) gives the source term that is recursive in the sense that the power in the previous time step is used along with the current power to calculate the reactivity. This value of S_i can be used for real-time calculation of reactivity with the help of (4). Denoting present and past values by subscript 1 and 0, respectively, we can write

$$\rho_1 = \beta + \frac{l^*}{P_1}\left(\frac{P_1 - P_0}{\Delta t}\right) - \frac{1}{P_1}\sum_{i=1}^{6} \beta_i \lambda_i S_{i1} \tag{12}$$

and

$$S_{i1} S_{i0} e^{-\lambda_i \Delta t} + \frac{1}{\lambda_i}\left(1 - e^{-\lambda_i \Delta t}\right)\left[P_0 - \frac{P_1 - P_0}{\lambda_i \Delta t}\right] + \frac{P_1 - P_0}{\lambda_i}. \tag{13}$$

The initial value of S_i is calculated from the mean power level at which the reactor is assumed to be critical:

$$S_{i0} = \frac{\langle P_0 \rangle}{\lambda_i}. \tag{14}$$

Equation (12) is the well-known inverse kinetic equation. The following observations must be made about this equation. First of all, it is nondimensional in $P_{(t)}$. Secondly, $P_{(t)}$ must have a physically acceptable behavior, i.e., $P_{(t)} = 0$ for all t.

An interesting aspect of kinetic equations solution is the value of the initial reactivity returned by these equations at $t = 0$. Substituting the value of S_{i0} from (14) in (4), the first and third terms cancel out since they are equal in magnitude and opposite in sign. Also, since $dP0/dt = 0$, the second term of (4) is equal to zero. The first (initial) value of the reactivity obtained from the above equation will therefore always be zero, irrespective of the state of the reactor.

III. Description of Reactivity Meter

The reactivity meter designed for PARR reactors reads the neutron density signal from plant instrumentation in real-time and feeds this information to the algorithm for the calculation of reactivity. A block diagram of reactivity meter system for PARR-1 is shown in Fig. 1. The data acquisition and processing is performed by the PDP 11/23 Plus plant computer. One feature of the data acquisition scheme is that the system can select any one of the nuclear flux channels' signals in the reactor by simple software command. For PARR-2, which is a small 27-kW miniaturized neutron source (MNSR) reactor, the reactivity meter is developed on an IBM PC/AT. Two options are available for signal acquisition. The first is a 12-bit analog-to-digital converter (ADC) card with 16 input

analog signals. The second option is a locally developed pulse acquisition card, which features 16-bit count resolution and fast sampling rate on a maximum of 8 pulse signals [5].

In the ensuing sections the details of data acquisition and processing for the more complex PARR-1 reactivity meter are described.

A. Data Acquisition

The data acquisition part of the reactivity meter at PARR-1 is similar to the normal plant signal monitoring system described elsewhere [6]. The analog output from the neutron flux monitoring channels is in the form of $0 \cdots 20$ mA current signal. This current output is transformed into $0 \cdots +5$ V output and fed to the analog I/O boards AXV11-C of PDP 1123-plus computer for analog-to-digital conversion. Signal conditioning prior to the computer input is performed to suppress noise. The AXV11-c card has one analog-to-digital converter with 12-bit data resolution and accepts a maximum of 16 input signals. Two digital-to-analog converters (DAC's) are also available on the card, which can convert the 12-bit digital data into ± 10 V analog output.

B. Algorithm for Reactivity Calculation

The computer program for reactivity calculation uses two levels of programming. One is the lower-level Assembler macro named REACMAC, which performs a dialogue with the machine for all data acquisition and I/O functions on analog-to-digital signals. The other routine is a Fortran-77 program REACFOR, which reads the digitized data acquired by REACMAC and uses them for the calculation of reactivity based on the formalism described in Section II (equation (12)). The smoothing of digitized input data is also performed in this routine using the moving average method [7].

The two programs REACMAC and REACFOR are initiated simultaneously, and they operate interactively with each other via a common block named 'ANALG'. The transfer of control from one program to another is by setting or clearing certain event flags. The control logic of these programs is shown in Fig. 2. The routine REACMAC (program A) generates the addresses of the ADC and DAC units and selects the particular input reactor power signal to be monitored. It also generates the sampling interval or the time delay (Δt) between two successive data samples. After the completion of analog-to-digital conversion, the digitized value of input signal is loaded into the common block ANALG. REACMAC then transfers control to the Fortran program (B) by setting the event flag FB and goes into the wait mode. REACFOR reads the value of input data from the common block, performs digital smoothing of data, and converts it into actual reactor power value.

For an accurate estimate of initial reactor power, the program simply averages the input data for the first 50 steps. Once the time average reactor power is obtained, program B uses instantaneous power $P_{(t)}$ to calculate reactivity. After the reactivity calculation, program A is again reactivated, which displays the digital reactivity data into analog form with the help of the digital-to-analog converter.

Once the cycle of reactivity calculation and display is complete, programs A and B jump to the start of the loop for new reactivity computation. The programs can be stopped by giving the appropriate stop command from the operator console. The last value of reactivity before program halt is stored in the DAC data register and can be continuously displayed. The cycle time for one complete reactivity step is set at 0.3 s for PARR-1 and 0.5 s for PARR-2. Experimental measurements have shown that this time is short enough to measure fast reactivity transients in the two reactors [8].

IV. Results

A. Selection Criteria of the Input Signals

Since the reactivity meter requires neutron density data as an input, it is essential to select a proper input signal from the variety of neutron detectors installed around the reactor core. Logarithmically amplified neutron flux signal is recommended for reactivity calculation [9] since an exponential variation in neutron flux between two successive time steps can be approximated by a straight line. In order to determine the effect of various types of neutron flux signals, reactivity calculations were made at steady-state reactor power with the help of start-up, linear, and logarithmic flux channels of standard reactor instrumentation in PARR-1. The percent root mean error (σ) of the input power signals and reactivity data was calculated in each case. The largest error of the input signal was observed for pulse-type start-up channels (about 4% of the mean count rate). The logarithmic channel signal gave an error of less than 1%. The five-point smoothing of the data further reduced this error to about 0.6%.

As will be explained in later sections, for most of the cases, the relatively slow response of the logarithmic amplifier did not affect the ability to measure fast reactivity changes in the reactor. Based on these measurements the logarithmic channel B signal was selected for reactivity monitoring at PARR-1. Another advantage of this channel signal was that its detector was placed at the opposite end of the core with respect to the external neutron source. Pulse or linear flux signals were also used in some cases to determine fast reactivity transients.

B. Initial Calibration of Reactivity Meter

As explained in Section II, the initial reactivity computed by the reactivity meter will always be zero, irrespective of the actual state of the reactor. It is therefore essential to calibrate the reactivity meter by accurately determining the initial reactivity of the reactor with the help of some independent method. At PARR reactors this is accomplished by the inverse kinetic rod drop method (IKRD), which has been installed on an IBM PC/AT [10]. The IKRD can determine precisely the initial reactivity for any subcritical or near critical state. This method is used to calibrate the reactivity meter at both reactors for any particular initial position of the shim rod bank, or whenever there is any change in the operating core conditions.

C. Reactivity Determination During Approach to Full Power

In order to demonstrate the prompt response of reactivity meter, the reactor power and reactivity plots during the

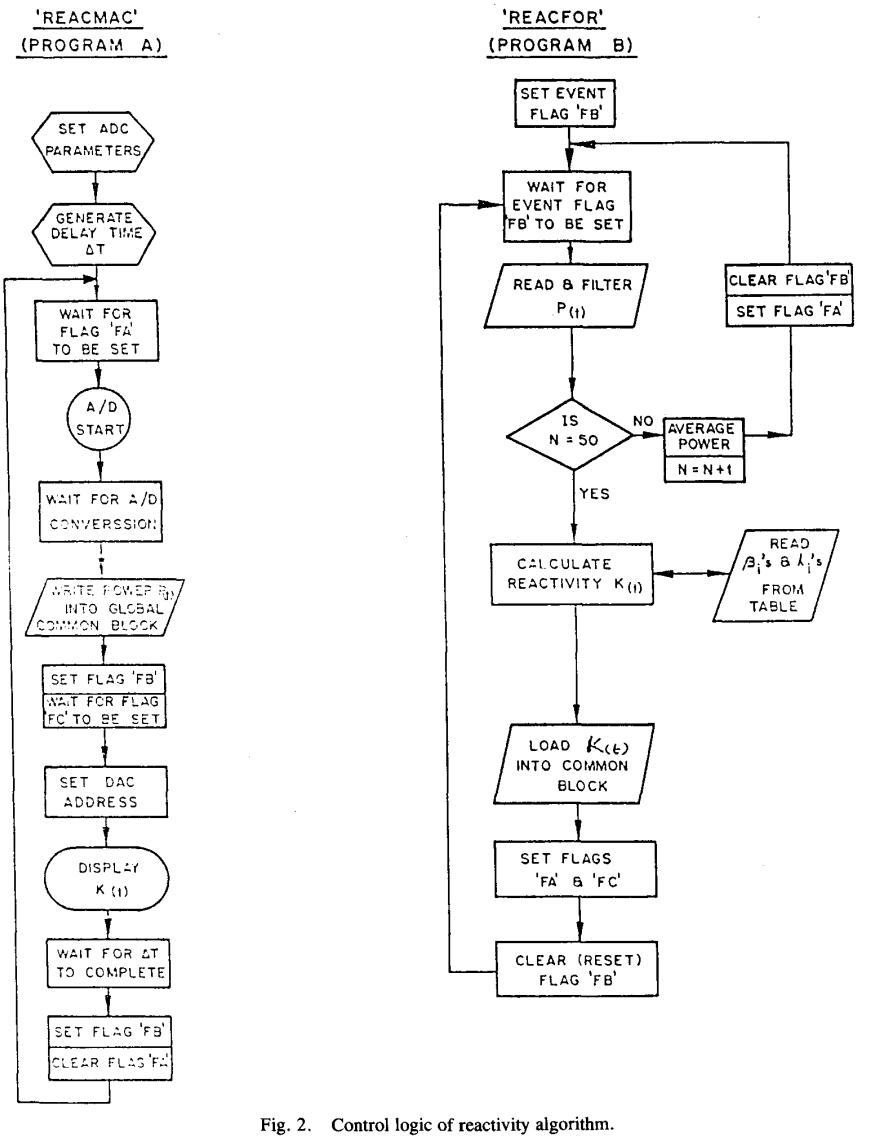

Fig. 2. Control logic of reactivity algorithm.

approach to full power of a particular run of PARR-1 reactor are shown in Fig. 3. The reactor power was raised in steps and the power and reactivity meter output was plotted. The reactor power was initially stable at 500 kW till time $t1$ when a fast positive reactivity insertion was introduced in the core by withdrawing all control rods. Between time $t2$ and $t3$ the system reactivity was undisturbed. At time $t3$ negative reactivity was introduced by inserting the control rods in the core, and the reactor was brought back to critical. In curve A of Fig. 3, the reactivity fluctuates around zero till time $t1$. Between time $t1$ and $t2$ curve A shows a jump of 0.08% $\Delta K/K$ and levels off at this value until time $t3$ when the reactor reestablishes itself at the new critical state around 0.005% $\Delta K/K$. After about 100 s from the start of the measurements, another positive reactivity insertion was made and the reactor power was allowed to attain the rated maximum power level around 4.5 MW. The resulting reactivity and power behavior is represented in the later parts of curves A and B of Fig. 3.

The following facts are evident from Fig. 3.

1) The response of the reactivity meter to any change in system reactivity is prompt within the sampling time delay (0.2 s) of the power signal.
2) The behavior of reactor power is markedly different from the reactivity behavior, and it is impossible to obtain an idea about the state of the reactor from curve B.

D. Control Rod Worth Determination

Determination of control rod reactivity worth is of fundamental safety importance since all reactivity control in the reactor is accomplished by means of control rod manipulation. The control rod worth of individual rods in the two

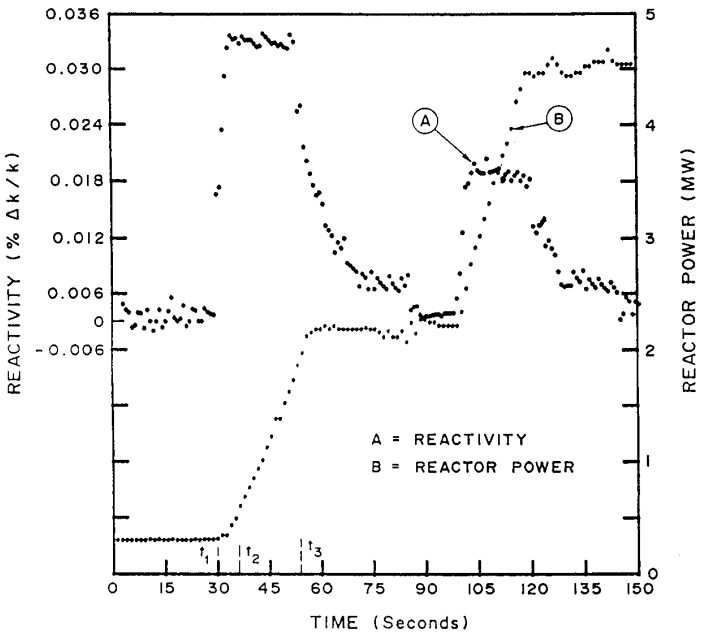

Fig. 3. Reactivity and power plots for full power run.

TABLE I
COMPARISON OF INTEGRAL ROD WORTH FOR INDIVIDUAL CONTROL RODS IN PARR-1 OBTAINED BY DIFFERENT METHODS

.Control Rod Number	Integral Worth ($-\%\Delta k/k$) Reactivity meter	IKRD	In-hour	Initial Reactivity ($-\%\ \Delta k/k$)
1	1.378	1.381	1.390	0.003
2	2.466	2.680	2.410	0.312
3	1.580	1.530	1.562	0.015
4	1.693	1.824	1.696	0.247
5	3.342	3.242	3.322	0.006
PARR-2				
1	0.725	0.710	—	0.017

reactors was determined by dropping one rod from the fully out position and measuring the system initial and final reactivity. The difference of the two reactivities gave the integral rod worth. The values of rod worth in both reactors were measured by the IKRD method, the reactivity meter, and the stable period (in-hour method) [2]. These values are presented in Table I along with the system initial reactivity. Note that for those cases where the reactor was initially subcritical, the reactivity meter gave a higher estimate of rod worth because it assumed the initial reactivity to be zero. One advantage of the reactivity meter over the IKRD method is that it works for both negative and positive reactivity changes, whereas the IKRD is valid for negative reactivities alone. This feature of the reactivity meter can be put to use for the determination of differential rod worth in which a rod is withdrawn by a small amount and the resulting positive reactivity is measured. An extension of the above measurements is the determination of positive reactivity worth of the new fuel and reflector elements added to the core, which can be measured very effectively by the reactivity meter.

E. Determination of Reactivity Worth of In-core Samples

In another application of the reactivity meter the reactivity worth determination of the irradiation samples around the reactor core was measured in PARR-1. The sample worth must be determined accurately to give the reactor operator an idea about the margin of positive reactivity needed to compensate for parasitic neutron absorption. A cadmium sample weighing 4.5 g was placed near the reactor core with reactor operating at the full power level of 5 MW. The effect of sample loading on the system reactivity is shown in Fig. 4. Before the sample loading, reactor power was leveled and reactivity varied around 0.005% $\Delta K/K$ with zero mean value. As the sample was loaded at time $t1$, the reactivity promptly dropped to 0.025% $\Delta K/K$ and leveled off at this new value. At time $t2$ the sample was removed from the reactor core by moving it vertically upward, and the reactivity assumed the new stable value around zero. The effect of sample oscillation on system reactivity is shown in the latter part of the curve, beyond time $t3$.

F. Determination of Reactivity Coefficient

In order to determine the time-dependent negative reactivity insertion in the core by temperature and poison effects, the reactivity meter output was collected for about one half hour immediately after attaining full reactor power. During this period the reactor power was allowed to vary on its own without any operator or auto-controller action. The reactor power registered a decrease of about 20% in 30 min time. The behavior of system reactivity as a function of time is plotted in Fig. 5. The time interval between two successive points of Fig. 5 is not fixed but adjusted according to the time when the Log N channel registered a change in the neutron flux value. The above measurements yielded a total power coefficient of reactivity in PARR-1 as −0.105 mk/h.

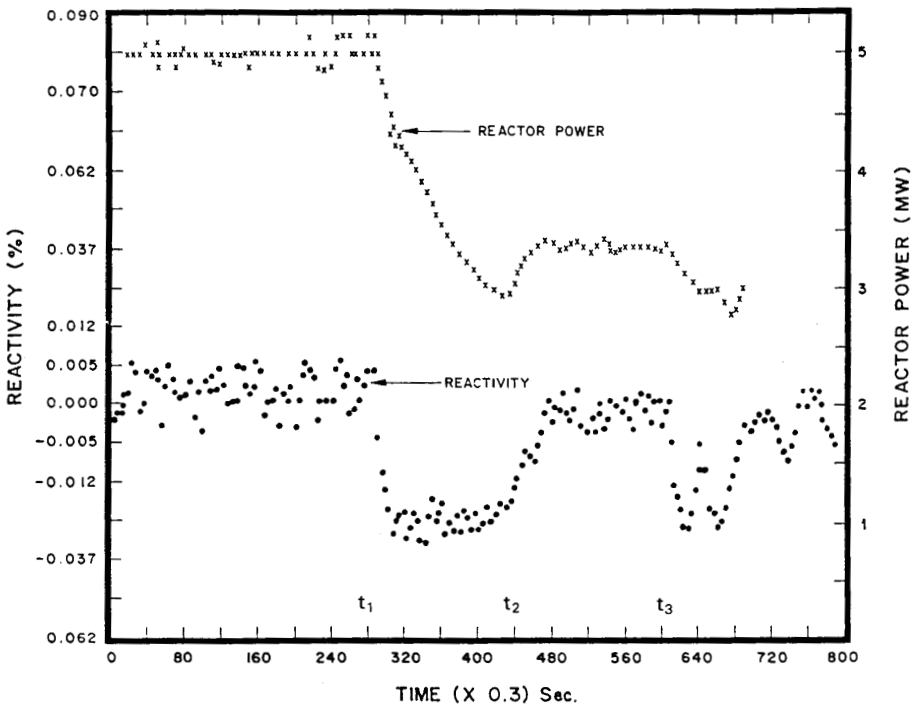

Fig. 4. Effect of Cadmium sample loading on system reactivity and power.

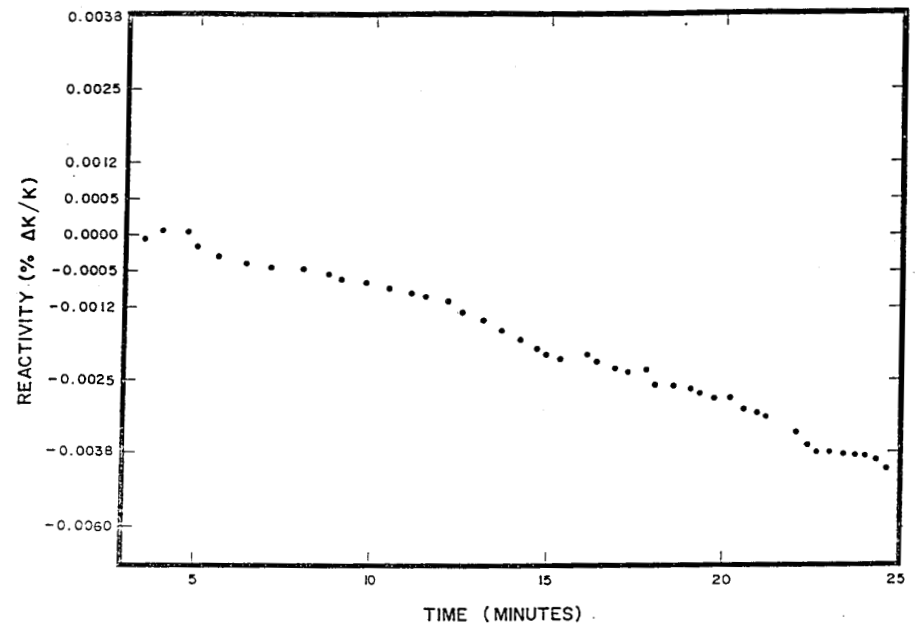

Fig. 5. Reactivity coefficient determination of PARR.

G. Determination of Reactor Auto-Controller Characteristics

In order to determine the effect on the system reactivity of the closed-loop proportional–integral–differential (PID) controller of the reactor, a comparison was made between the reactivity data obtained in the manual and auto-control mode of reactor operation. The reactor was operated at lower power level to eliminate any external reactivity disturbance like poison and temperature in both modes. The behavior of system reactivity as a function of time in auto-control mode is shown in Fig. 6. As is evident from the figure, the auto-controller maintains system reactivity within 0.1 mk in the absence of external disturbances. The controller action is also free of any in-built reactivity oscillations.

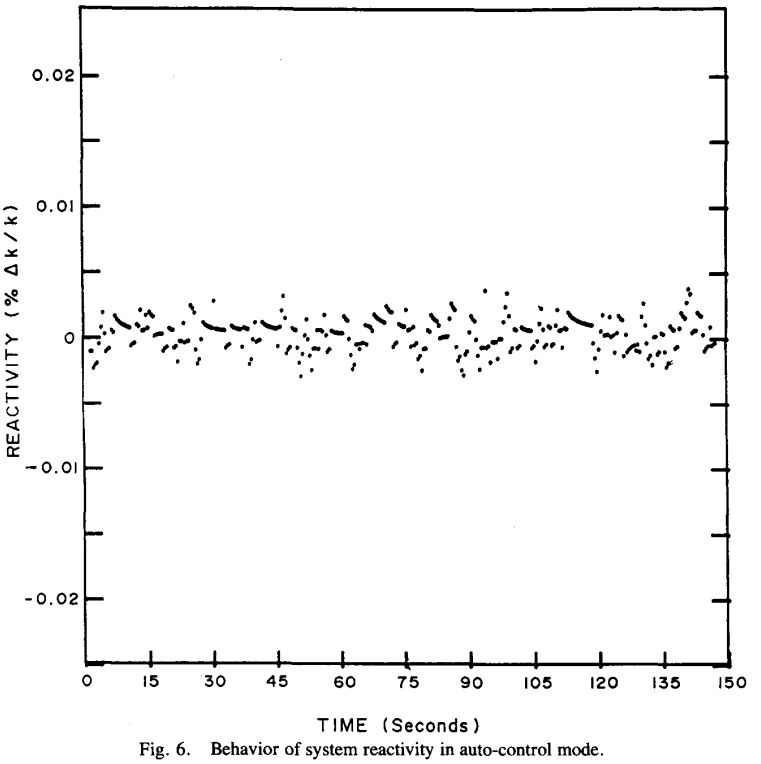

Fig. 6. Behavior of system reactivity in auto-control mode.

Conclusion

As described in this paper, the system of a digital reactivity meter developed on a PDP-1123 minicomputer and the personal computer proved to function satisfactorily in the nuclear reactor. The utilization of the plant signals makes the system simple and economic. The reactivity meter would be a useful tool in the commissioning of the new core of the PARR-1 reactor, which is being upgraded to 10 MW and converted to low enriched uranium fuel.

References

[1] S. E. Binney and A. J. M. Bakir, "Design and development of a personal-computer-based reactivity meter for a research reactor," *Nucl. Tech.*, vol. 85, pp. 12–21, Apr. 1989.

[2] E. Profio, *Experimental Reactor Physics*. New York: Wiley, 1976.

[3] O. Ciftcioglu and M. Geckinli, "A CAMAC based reactivity-meter for nuclear reactors," *Nucl. Instrument. Methods*, 177, pp. 321–326, 1980.

[4] J. Lamarsh, Introduction to Nuclear Reactor Theory. New York: Addison-Wesley, 1966.

[5] B. Majid, Z. Ahmad, and A. Usman, "Design of multiple channel counting system for IBM PC/XT/AT and compatible," PINSTECH Rep. to be published.

[6] A. Karim, *et al.*, "Renovation of PARR instrumentation and controls," PINSTECH-109, Jan. 1987.

[7] A. Savitzky and M. Golay, "Smoothing and differentiation of data by simplified least squares procedures," *Anal. Chem.*, vol. 36, no. 8, pp. 1627–1639, July 1964.

[8] S. A. Ansari, "Development of on-line reactivity meter for PARR," PINSTECH-111, June 1988.

[9] G. Steffen, "A portable digital reactivity meter for power reactors," *Kerntechnik 19*, no. 7, pp. 327–332, 1977.

[10] S. A. Ansari, B. Majid, and A. Hussain, "Development of a personal-computer-based system for control rod worth determination in a nuclear reactor," *IEEE Trans. Nucl. Sci.*, vol. 35, no. 5, pp. 2149–2155, Dec. 1990.